

# Stochastic resonance and noise-enhanced transmission of spatial signals in optics: the case of scattering

Fabrice Vaudelle, José Gazengel, and Geneviève Rivoire

*Laboratoire des Propriétés Optiques des Matériaux et Applications, IUT, Université d'Angers,  
4 Boulevard Lavoisier, 49000 Angers, France*

Xavier Godivier and François Chapeau-Blondeau

*Laboratoire d'Ingénierie des Systèmes Automatisés, Faculté des Sciences, Université d'Angers,  
2 Boulevard Lavoisier, 49000 Angers, France*

Received December 3, 1997; revised manuscript received April 14, 1998

The nonlinear effect of noise-enhanced signal transmission by means of stochastic resonance in optics is studied. We investigate this effect for the novel case of spatial signals or images. With a theoretical model involving a threshold nonlinearity we describe a mechanism whereby the transmission of an image can be improved by the addition of noise. We argue that such a nonlinear mechanism can operate in different types of light scattering. With a stimulated Raman scattering experiment we verify the existence of a stochastic resonance effect in the transmission of a laser image; we show that maximal efficacy is obtained with the assistance of a speckle of sufficient intensity. The results extend the scope of stochastic resonance and can serve as a basis for further development of the effect in optics. © 1998 Optical Society of America  
[S0740-3224(98)00310-5]

OCIS codes: 070.4340, 100.0100, 110.2970, 030.4280, 190.0190, 190.5650.

## 1. INTRODUCTION

A nonlinear phenomenon, known as stochastic resonance, is gradually attracting increasing attention from researchers in various scientific fields.<sup>1,2</sup> In general terms, stochastic resonance can be described as an improvement of the transmission of a signal by certain nonlinear systems, which results from the addition of noise to the system. The paradoxical phenomenon was formally introduced some 17 years ago in the context of climate dynamics,<sup>3</sup> although some aspects of the effect can be traced back further.<sup>4</sup> Since its introduction, stochastic resonance has developed considerably, as it was progressively observed in an increasing variety of processes, including electronic circuits, optical systems, mechanical motions, magnetic devices, chemical reactions, and neurons.<sup>5,6</sup>

In the light of the recent results, it appears that stochastic resonance can appear in various forms, depending on the type of ordered or information-carrying signal, of noise, and of nonlinear system of transmission and on the measure of efficacy receiving improvement from the noise. An important form of this phenomenon that is frequently considered involves a bistable dynamic system governed by a double-well potential, in which a periodic signal receives assistance from the noise to overcome the potential barrier and switch the system between its two stable states. This is the form in which stochastic resonance was first reported<sup>3</sup> and in which it has received the greatest attention,<sup>1,6-8</sup> as such periodically driven double-well dynamics were shown to apply to a wide variety of physi-

cal processes. In this case of a periodic signal, the common measure of stochastic resonance is a signal-to-noise ratio (SNR) that quantifies, in the system response, the power at the frequency of the periodic drive relative to the power in the noise fluctuation.<sup>1,2,6</sup> The signature of stochastic resonance is a SNR that culminates in a maximum value for an optimal (nonzero) noise level. In this nonlinear context of periodically driven bistable dynamic systems, theoretical analyses of stochastic resonance have been proposed, especially to predict the behavior of the SNR; they usually resort to approximations and are frequently restricted to the case of a slow or a small periodic signal or both.<sup>5-7,9</sup> Recent advances that are especially significant for practical applications, include the extension of stochastic resonance for the transmission of aperiodic signals, for which case new measures of efficacy (because the conventional SNR no longer applies) have been proposed and shown to be improvable by the addition of noise.<sup>10,11</sup>

For the domain of optics, stochastic resonance has been reported in the context of periodically driven bistable dynamic systems, for which several implementations have been proposed to realize a bistable optical system that is switched between its two stable states by a periodic signal (usually a sinusoid) aided by noise.<sup>1,2,6</sup>

Recently a theory was proposed<sup>12</sup> that describes stochastic resonance in another class of nonlinear dynamic systems (other than double-well bistable dynamics) in which the nonlinearity is static (or memoryless) and possibly followed by an arbitrary linear dynamic system.

This theory demonstrates that stochastic resonance can occur in simple nonlinear systems, as simple as a threshold nonlinearity, for instance. This form of stochastic resonance with threshold or static nonlinearities has also been found applicable to a wide variety of physical systems,<sup>13,14</sup> including electronic circuits<sup>15</sup> and neurons.<sup>16</sup> One of our purposes in writing this paper is to demonstrate its feasibility in optical settings, especially in different types of light scattering in which a noise-enhanced signal transmission can be obtained.

Another important feature shared by the optical systems (and by most other systems also) that have been shown to exhibit the double-well-dynamics form of stochastic resonance is that they deal with temporal or one-dimensional signals. By contrast, the more recent form of stochastic resonance with static nonlinearities<sup>12</sup> can readily be extended to spatial or two-dimensional signals as encountered in optics with images. It is another purpose here to discuss the possibility of noise-enhanced transmission through stochastic resonance for spatial signals in optics. Application of stochastic resonance to spatial signals is a new topic, seldom considered except in a recent study that reports a psychophysical experiment showing that visual perception of images can be improved by addition of noise.<sup>17</sup>

We first present a mechanism for stochastic resonance in a simple static nonlinearity operating on aperiodic spatial signals, together with the establishment of a measure of efficacy appropriate for this novel context. We then show that such a mechanism can be expected to operate, at least approximately, in optical systems that involve scattering of light. We then report results from a stimulated Raman scattering experiment that demonstrate a stochastic resonance effect with spatial signals.

## 2. MODEL FOR STOCHASTIC RESONANCE IN SPATIAL SIGNALS

Let  $S(x, y)$  be a binary image, where  $(x, y)$  are integers that index the pixels on the array with  $S(x, y) = 0$  or  $S(x, y) = 1$ . A noise  $N(x, y)$  corrupts linearly each pixel of image  $S(x, y)$ . The noise values are independent from pixel to pixel and are identically distributed with the cumulative distribution function  $F(u) = \text{Pr}[N(x, y) \leq u]$ . The sum  $S(x, y) + N(x, y)$  is input onto a nonlinear system, producing the output  $Y(x, y)$  according to the following expressions:

$$\begin{aligned} \text{If } S(x, y) + N(x, y) > \theta, \text{ then } & Y(x, y) = 1, \\ \text{else} & Y(x, y) = 0. \end{aligned} \quad (1)$$

We consider the regime where the threshold  $\theta > 1$ . In this condition and in the absence of noise  $N(x, y)$ , input image  $S(x, y)$  alone is totally unable to trigger a response in  $Y(x, y)$ , which remains a blank image (filled with zeros), and input pattern  $S(x, y)$  is completely lost in output  $Y(x, y)$ . Then, if noise  $N(x, y)$  is gradually raised above zero, there will first exist a possibility of cooperation in which the noise can assist the bright pixels  $S(x, y) = 1$  in overcoming the threshold to light on a response  $Y(x, y) = 1$  on the output image. This beneficial outcome first gets more probable as the noise level is increased, reinforcing the similarity of output image  $Y(x, y)$  and input image  $S(x, y)$ . Past an optimum level when the noise is further raised, the action of noise  $N(x, y)$  alone tends to dominate output image  $Y(x, y)$ , which ends up with a random appearance. In this way, if input image  $S(x, y)$  contains a pattern with spatial correlation, this pattern will be transferred to the output image with assistance from the noise, and with maximum efficacy for an optimal noise level, as illustrated in Fig. 1.

The present mechanism, in common with other forms of stochastic resonance, achieves a noise-enhanced signal transmission. This mechanism, compared with the standard forms of stochastic resonance, includes two unique features. First, it deals with an aperiodic rather than a periodic input signal; second, it involves spatial (two-dimensional) rather than temporal (one-dimensional) signals. To quantify the effect here, the SNR defined in the frequency domain for periodic temporal signals is no longer appropriate, because for aperiodic spatial signals the information involved has no precise frequency localization. We propose to extend here to spatial aperiodic signals, correlation measures similar to those introduced in Ref. 10 for stochastic resonance with temporal aperiodic signals. To quantify the visual effect that appears in Fig. 1 we need a quantitative measure of the similarity between input image  $S(x, y)$  and output image  $Y(x, y)$ , and we need to show that this measure culminates at a maximum value for an optimal nonzero noise level. A possible measure is the normalized cross correlation between images  $S$  and  $Y$ , defined as

$$R_{SY} = \frac{\langle SY \rangle}{\sqrt{\langle S^2 \rangle \langle Y^2 \rangle}}, \quad (2)$$

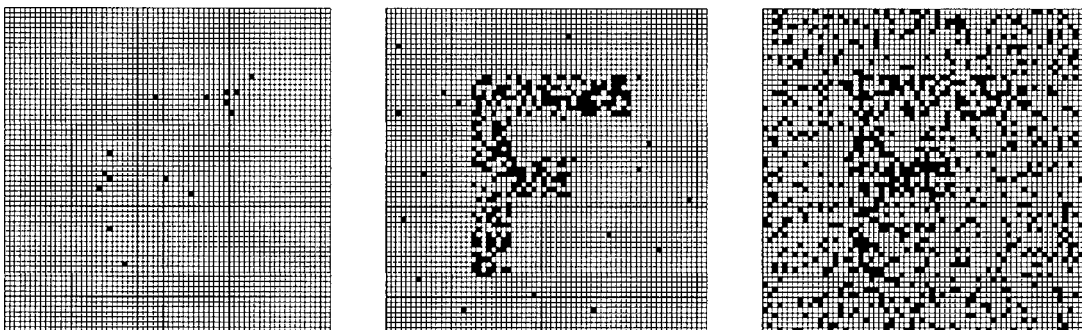


Fig. 1. Output  $64 \times 64$  image  $Y(x, y)$  after transmission according to expressions (1) with  $\theta = 1.1$ . The binary input image  $S(x, y)$  represents the letter  $F$ , and  $N(x, y)$  is zero-mean Gaussian noise with rms amplitudes 0.05 (left), 0.43 (center), and 1 (right).

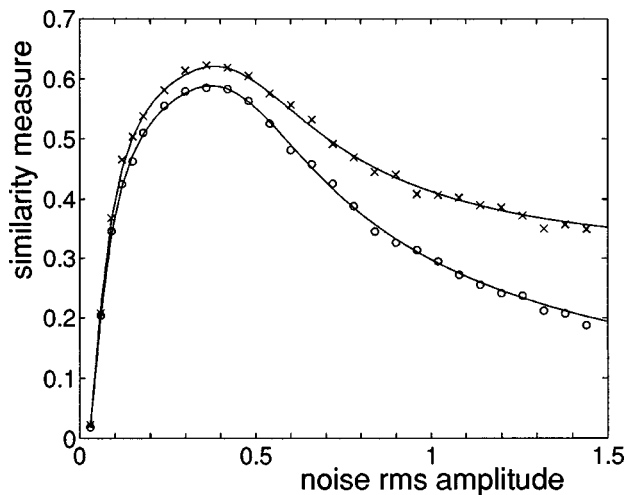


Fig. 2. Similarity between input image  $S(x, y)$  and output image  $Y(x, y)$  as a function of the input noise rms amplitude under the conditions of Fig. 1 with probability  $p_1 = 0.148$ . Solid curves, theoretical expressions of the cross correlation  $R_{SY}$  of Eq. (7) (upper trace) and the cross covariance  $C_{SY}$  of Eq. (8) (lower trace). The two sets of discrete data points are experimental estimations through pixels counting on images.

where  $\langle \rangle$  denotes an average over the images. A strong similarity between images  $S$  and  $Y$  is denoted by  $R_{SY}$  close to 1.  $R_{SY}$  quantifies the similarity contained both in the mean values of the images and in the fluctuations around these means. It is also possible to measure the similarity contained only in the fluctuations around the means, with the normalized cross covariance

$$C_{SY} = \frac{\langle (S - \langle S \rangle)(Y - \langle Y \rangle) \rangle}{[\langle (S - \langle S \rangle)^2 \rangle \langle (Y - \langle Y \rangle)^2 \rangle]^{1/2}}, \quad (3)$$

where  $C_{SY}$  is close to 1 when images  $S$  and  $Y$  carry strongly similar structures and is close to 0 when the images are unrelated.

We now derive theoretical expressions for our similarity measures  $R_{SY}$  and  $C_{SY}$ , as a function of the statistical properties of noise  $N$ , and show that both of them are able to verify the presence of stochastic resonance.

We have the average  $\langle S \rangle = 1 \times \Pr(S = 1) + 0 \times \Pr(S = 0)$ ; thus  $\langle S \rangle$  is simply  $p_1 = \Pr(S = 1)$ , the probability of a pixel at 1 in image  $S(x, y)$ , which can be estimated as the fraction of pixels at 1 in a large image. In the same way  $\langle Y \rangle = \Pr(Y = 1) = q_1$ , where this new probability  $q_1$  is expressible as

$$q_1 = p_{11} \times p_1 + p_{10} \times (1 - p_1). \quad (4)$$

We have introduced the conditional probability  $p_{11} = \Pr(Y = 1|S = 1)$ , which is also  $\Pr(S + N > \theta|S = 1)$ , which amounts to  $\Pr(N > \theta - 1) = 1 - F(\theta - 1)$ . With similar rules we arrive at

$$p_{11} = \Pr(Y = 1|S = 1) = 1 - F(\theta - 1), \quad (5)$$

$$p_{10} = \Pr(Y = 1|S = 0) = 1 - F(\theta). \quad (6)$$

Also, we have  $\langle SY \rangle = 1 \times 1 \times \Pr(Y = 1; S = 1) = p_{11}p_1$ .

The numerator of Eq. (3) is expressible as  $\langle SY \rangle - \langle S \rangle \langle Y \rangle$ . The denominator of Eq. (3) is nothing more than the product of the standard deviations  $SD(S)$

$\times SD(Y)$ , with  $[SD(S)]^2 = \langle S^2 \rangle - \langle S \rangle^2$  and  $\langle S^2 \rangle = 1^2 \times \Pr(S = 1) + 0^2 \times \Pr(S = 0) = p_1$ . Also,  $[SD(Y)]^2 = \langle Y^2 \rangle - \langle Y \rangle^2$ , with  $\langle Y^2 \rangle = q_1$ . Collecting these results, we obtain for the cross correlation of Eq. (2)

$$R_{SY} = \frac{p_{11}p_1}{\sqrt{p_1q_1}} \quad (7)$$

and for the cross covariance of Eq. (3)

$$C_{SY} = \frac{p_{11}p_1 - p_1q_1}{[(p_1 - p_1^2)(q_1 - q_1^2)]^{1/2}}. \quad (8)$$

Our two similarity measures to characterize stochastic resonance,  $R_{SY}$  and  $C_{SY}$ , are now completely computable, through Eqs. (4)–(6), for a given  $p_1$  as a function of the noise properties conveyed by  $F(u)$ .

Figure 2 shows the evolution, with the noise rms amplitude, of our two similarity measures provided by the normalized cross correlation  $R_{SY}$  and the cross covariance  $C_{SY}$  in the conditions of Fig. 1, where the probability  $p_1 = 0.148$ . Both measures exhibit a nonmonotonic evolution that culminates at a maximum for an optimal non-zero noise level. The noise level that maximizes  $R_{SY}$  and  $C_{SY}$  also corresponds to the maximum visual similarity that one can get when observing the images of Fig. 1, which demonstrates an effect of noise-enhanced information transmission through stochastic resonance in spatial signals.

The results presented in this section are useful for two purposes: (i) They make clearly visible elementary ingredients (a subthreshold aperiodic signal assisted by noise to overcome a threshold nonlinearity) that can form the basis for a new form of stochastic resonance with aperiodic spatial signals and (ii) they establish measures appropriate to quantify the effect in this novel context. These results will now serve as guidelines for an experimental demonstration of this stochastic resonance.

### 3. STOCHASTIC RESONANCE WITH SPATIAL SIGNALS IN NONLINEAR OPTICS

We now investigate the possibility of a similar stochastic resonance effect in spatial signal transmission occurring in common phenomena of nonlinear optics. We look for optical processes that are able to couple an input signal with noise in a nonlinear manner appropriate to induce a noise-improved transmission. Light scattering by a nonlinear medium, as depicted in Fig. 3, is especially suited for this purpose. In the scheme of Fig. 3 the coherent input signal  $S$ , the input noise  $N$ , and the output  $Y$  can be light electric fields or light intensities. When it is analyzed in terms of nonlinear optics, Fig. 3 represents a typical two-wave mixing scheme. The beams that carry  $S$ ,  $N$ , and  $Y$  have transverse spatial structures forming

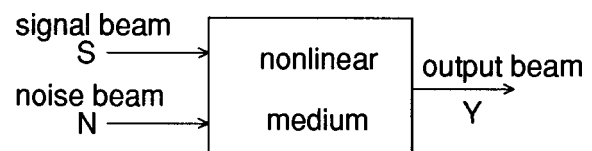


Fig. 3. Schematic of the interaction that nonlinearly couples a signal beam and a noise beam to produce an output beam.

images. We are interested in nonlinear phenomena able to couple beams  $S$  and  $N$  such that output beam  $Y$  (or at least one of the output beams induced by the coupling) reproduces accurately the spatial structure of input  $S$  with assistance from noise  $N$ .

In general, the nonlinear coupling of the two inputs can be implemented by a material that exhibits either a second- or a third-order nonlinearity. In both cases we can consider the use of the real or the imaginary part of the nonlinear susceptibility. Third-order phenomena yield a favorable variety of two-field coupling modes and are considered first. For two incident beams with the same spectral frequency  $\omega$ , third-order coupling can be realized according to three kinds of physical process<sup>18</sup>:

- The first one is the nonlinear variation of the material refractive index, described by the real part of the third-order nonlinear susceptibility without frequency change:  $\chi(\omega; \omega, \omega, \omega)$ . It characterizes parametric coupling in which energy transfers between the beams occur without losses in the nonlinear medium.

- The second makes use of a nonlinear absorption—saturable or inverse saturable—described by the imaginary part of  $\chi(\omega; \omega, \omega, \omega)$ . In this case, energy can be exchanged among the beams and between the nonlinear medium and the beams.

- The third is stimulated scattering (Brillouin, Rayleigh, or Raman) described by the imaginary part of  $\chi(\omega_D; \omega, \omega, \omega_D)$ , where  $\omega_D$  is the stimulated scattering frequency related to the incident wave frequency by  $\omega_D = \omega \pm \Delta\omega$  and  $\Delta\omega$  characterizes the frequency change produced in the nonlinear medium by the scattering process. With stimulated Raman scattering,  $\Delta\omega$  is a molecular vibration frequency. Notice that in this case output beam  $Y$  has a frequency  $\omega_D$  that is different from the frequency  $\omega$  of incident beams  $S$  and  $N$ .

In these three types of interaction the electric fields  $E_S$  and  $E_N$ , respectively, associated with beams  $S$  and  $N$  create a nonlinear polarization  $P$ , which is the source of the output electric field  $E_Y$ . This polarization is

$$P = \sum_{\{i,j,k\}=\{S,N,Y\}} \chi(\omega_Y; \omega_i, \omega_j, \omega_k) E_i E_j^* E_k. \quad (9)$$

Notice that in Eq. (9) both fields and intensities (the latter expressed by the product  $E_i E_j^*$ ,  $i = j$ ) can be active.

We assume here that the propagation of the three beams  $S$ ,  $N$ , and  $Y$  occurs along the  $Oz$  axis. The images formed by the spatial structure of the beams are described by the transverse distributions of the fields, or at least of the intensities, in plane  $(x, y)$ . We want to examine the possibility for the spatial structure of output  $Y$ , described, say, by  $|E_Y(x, y)|$ , to reproduce with best accuracy the spatial structure of input  $S$ , described by  $|E_S(x, y)|$ , with the help of an optimal nonzero noise level on  $N$ . This would be a stochastic resonance effect in image transmission by means of light scattering.

As revealed by the previous studies reviewed in Section 1 and conducted on temporal signals, the nonlinearities that involve a threshold are especially suited (although they are not absolutely necessary<sup>12,19</sup>) to inducing stochastic resonance. Also, as shown by the model of Section 2, a simple threshold mechanism is able to produce

an extension of stochastic resonance to spatial signals. We are thus lead to ask whether, among the optical interactions described above, some of them involve some sort of threshold. For the stimulated scatterings, when the exciting wave intensity is continuously increased from zero the scattered wave goes abruptly from a spontaneous regime to a stimulated regime with a steep and strong growth in intensity. A stimulated scattering threshold can be defined in the case of Brillouin, Rayleigh, and Raman scatterings and has been the subject of theoretical models and of measurements.<sup>20–22</sup> We then examine, in an experiment with stimulated Raman scattering (SRS), whether a stochastic resonance effect is indeed possible in these conditions.

The principle of the experiment is the following: spatial input signal  $S$  and noise  $N$  (composed of spatial speckle) produced by the same laser source are superposed in a nonlinear medium. The signal intensity in  $S$  alone is too weak to produce SRS. Addition of noise  $N$  allows SRS to be induced. The evolution of the Raman output signal  $Y$  is observed as a function of the intensity of the noise. The image carried by the output Raman beam is compared with the input image on  $S$ , and we look for the maximum similarity between them that would occur for a nonzero intensity of the speckle image.

## 4. STOCHASTIC RESONANCE IN A RAMAN NONLINEAR SYSTEM

### A. Stimulated Raman Scattering

Before we report the details of the experiment and its results it is useful to emphasize the key characteristics on which we rely, of the Raman response of a medium to excitation by a single laser beam. A simplified expression of output Raman intensity  $I_R$  as a function of input laser intensity  $I_L$  is given in Ref. 23 as

$$I_R = \frac{\frac{\hbar c \omega_D}{V} [\exp(Gl) - 1]}{\frac{\hbar c \omega}{\sqrt{I_L}} \exp(Gl) - 1}, \quad (10)$$

with  $G = (I_L + \hbar c \omega_D / V)g$ , where  $g$  is the Raman gain and  $l$  is the depth of penetration in the scattering medium excited over volume  $V$ .

Equation (10) conveys the essential nonlinear features of the evolution of  $I_R$  as a function of  $I_L$ , as depicted in Fig. 4. Three different regions can be distinguished in the evolution of Fig. 4: I, at low input intensities  $I_L$  spontaneous emission alone occurs and produces a weak linear response  $I_R$ ; II, for sufficient  $I_L$  stimulated emission comes into play and leads to an exponential growth of  $I_R$  to high values; III, the saturation of the active medium occurs and stops the exponential growth of  $I_R$ , which reverts to being linear.

The steep and strong growth of the Raman intensity  $I_R$  between regions I and II is a type of nonlinear response that can be appropriate to generate a stochastic resonance effect, for which we now look.

## B. Experimental Setup

The setup that produces and combines the signal and the noise inputs is represented in Fig. 5. A 25-ps pulse is provided by a double-frequency mode-locked Nd:YAG laser (532 nm). A beam splitter separates the incident laser into two components: The reflected beam (carrying 10% of the total laser energy) is used to produce the signal beam, and the transmitted beam produces the noise. The rotation of a half-wave plate associated with a fixed Glan polarizer permits a fine energy control in each beam without changing the linear polarization.

The signal beam is spatially modulated by grid G2. Then its size is reduced with an afocal device (L3, L4) and focused by lens L5 onto the cell that contains the active Raman medium. The image imprinted by G2 in the transverse structure of the signal beam is shown in Fig. 6.

The noise beam is produced when the input beam crosses aberrative phase plate G1, which is associated with the afocal system (L1, L2), to reduce the beam size. Phase plate G1 can be considered a random distribution of pupils. When it is illuminated by coherent light, plate G1 yields, by diffraction in the transverse plane, a spatially random distribution of intensity or speckle.<sup>24</sup> A speckle image carried by the transverse structure of the noise beam is shown in Fig. 7.

Recombination of the signal and noise beams is achieved by a beam splitter, and the composite beam goes

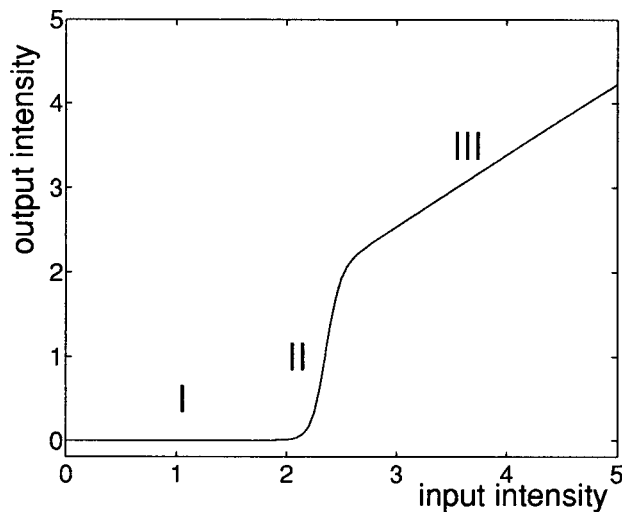


Fig. 4. Output Raman intensity  $I_R$  ( $\text{GW}/\text{cm}^2$ ) as a function of input laser intensity  $I_L$  ( $\text{GW}/\text{cm}^2$ ) as described by Eq. (10) with  $g = 10^{-11} \text{ m}/\text{W}$ ,  $l = 16 \text{ cm}$ , and  $V = 0.1 \text{ cm}^3$ .

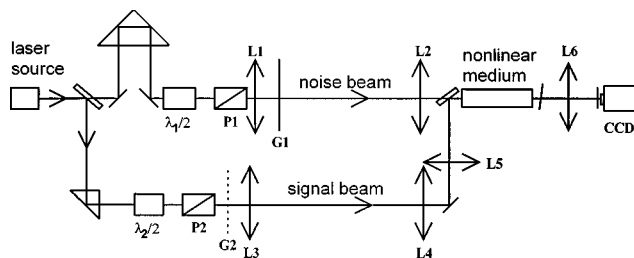


Fig. 5. Experimental setup:  $\lambda_1/2$ ,  $\lambda_2/2$ , half-wave plates; P1, P2, polarizers; L1, L2, L3, L4, L5, L6, lenses with foci, respectively, of 50, 10, 50, 15, 30, and 5 cm; G1, phase plate; G2, grid; NL, nonlinear medium; CCD, CCD camera.

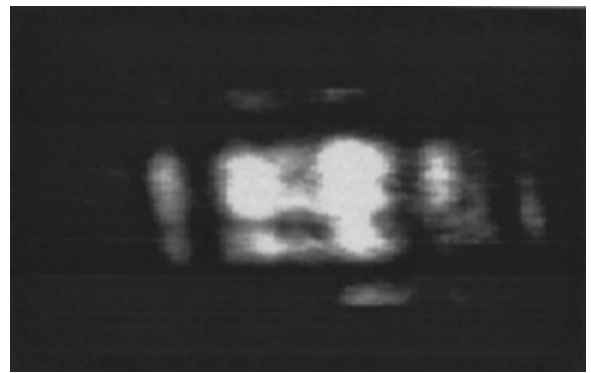


Fig. 6. Image carried by the transverse structure of the signal beam as it is observed on the CCD camera in the absence of both the nonlinear medium and the noise beam.

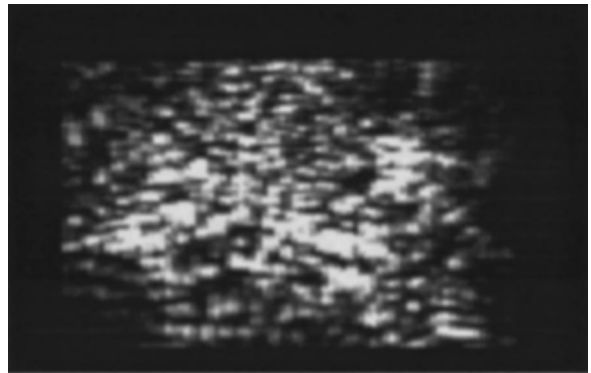


Fig. 7. Speckle image carried by the transverse structure of the noise beam as it is observed on the CCD camera in the absence of both the nonlinear medium and the signal beam.

through the Raman cell. The length  $l$  of the active medium contained in the cell is the result of a compromise. On the one hand,  $l$  has to be small enough to permit the same transverse distribution of the signal beam throughout the Raman medium; on the other hand,  $l$  has to be large enough to provide a sufficient forward Raman amplification and at the same time avoid backscattering.<sup>25</sup> Length  $l = 16 \text{ cm}$  is chosen when the active medium is a high-Raman-gain liquid such as acetone. Acetone is used in our experiment because it exhibits a large ratio of Raman gain/Kerr constant, which avoids perturbations by self-focusing. Moreover, its short Raman relaxation time (0.34 ps) ensures the steady-state exponential evolution of the scattering.

At the output of the cell the Raman wavelength (629 nm) is separated from the laser wavelength by a dichroic mirror and a selective filter. lens L6 (Fig. 5) focuses the Raman beam onto a CCD camera with a resolution of  $80 \times 60$  pixels with a  $16 \mu\text{m} \times 11 \mu\text{m}$  pixel size.

## C. Results

The intensity of the signal beam is adjusted below the Raman threshold (near  $2.5 \text{ GW}/\text{cm}^2$  in the acetone cell). In these conditions, in the absence of the noise beam (when the noise pathway is blocked), the signal beam alone is insufficient to induce SRS, and no output Raman image is detected on the CCD camera. The intensity  $I_N$  of the noise beam is then gradually increased from zero. For sufficient noise intensity, SRS produced by the superposi-

tion of the signal and noise beams inside the active medium begins to take place. An output image  $Y(x, y)$  is detected on the CCD camera and, as noise intensity  $I_N$  is raised further, we are interested in evaluating the similarity of output image  $Y(x, y)$  to input image  $S(x, y)$  carried by the input beam. A visual inspection can be performed with the images of Fig. 8. As noise intensity  $I_N$  is raised, the output image gradually becomes visible, and it emerges with increasing similarity to the input image. The maximum of similarity can be detected for the optimal noise intensity (Fig. 8e). As the noise intensity is raised further above this optimal level, the output image becomes increasingly dominated by the noise, and it

gradually loses its similarity to the input image. An optimal nonzero noise level then exists that maximizes the efficiency of the image transmission, which is the signature of a stochastic resonance effect.

For a quantitative characterization we computed the degree of similarity between input  $S(x, y)$  and output  $Y(x, y)$  images, defined by the cross correlation  $R_{SY}$  of Eq. (2). The evolution of  $R_{SY}$  with noise intensity  $I_N$  is shown in Fig. 9. Figure 9 clearly shows that the similarity measure  $R_{SY}$  begins to increase with noise intensity  $I_N$ , up to an optimal noise level where it is maximized, and then gradually decays with  $I_N$ . This is the quantitative confirmation of the stochastic resonance effect.

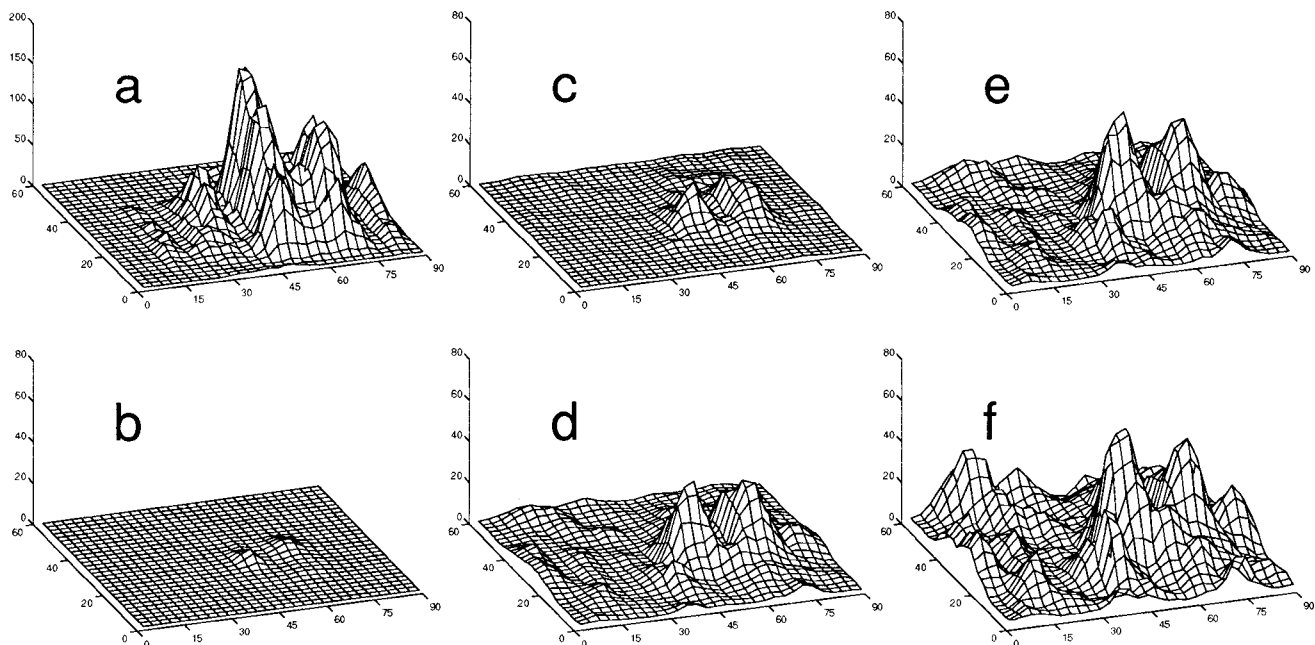


Fig. 8. a, Input image carried by the signal beam. b–f, Output Raman images obtained with the signal beam added to a speckle of increasing intensities  $I_N$  of b, 0.30; c, 0.36; d, 0.39; e, 0.41; f, 0.43  $\text{GW}/\text{cm}^2$ . Cross-correlation measure  $R_{SY}$  identifies the maximum similarity between the input and output images in e.

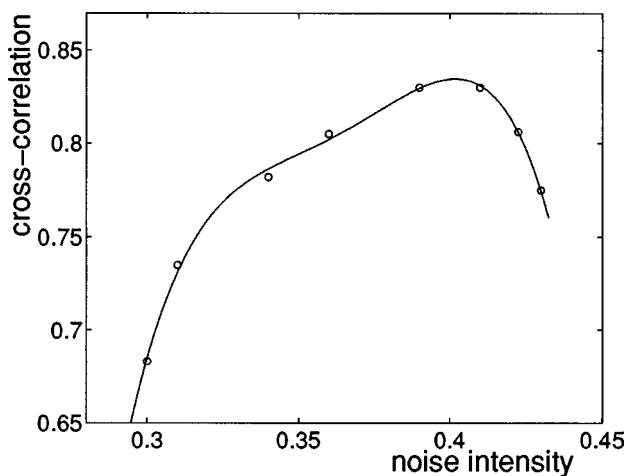


Fig. 9. Similarity between the input and output images defined by the cross correlation  $R_{SY}$  of Eq. (2) as a function of noise intensity  $I_N$  ( $\text{GW}/\text{cm}^2$ ). Circles, experimental data; solid curve, an interpolation.

## 5. DISCUSSION AND CONCLUSION

We have established, both with the theoretical model of Section 2 and with the SRS experiment of Section 4, the possibility of improving the nonlinear transmission of a spatial signal by adding noise.

The model of Section 2 presents the possibility of a form of stochastic resonance in the novel field of nonlinear transmission of spatial aperiodic signals. This simple model makes clearly visible the ingredients that render possible a stochastic resonance effect: (1) a nonlinear system that responds with a threshold or at least a sufficiently abrupt demarcation in its input–output transfer, (2) a signal that alone is insufficient to induce a significant response of the system, and (3) a noise that can assist the signal in overcoming the nonlinearity. The model of Section 2 also establishes quantitative measures appropriate for characterizing this novel form of stochastic resonance with spatial aperiodic signals.

We argued in Section 3 that the ingredients described

in Section 2 to induce stochastic resonance can be found in different types of light scattering by nonlinear media. We chose to examine the case of stimulated Raman scattering, and we conducted an experiment to demonstrate the possibility of stochastic resonance in spatial signal transmission. This experiment represents the first demonstration to our knowledge of a noise-enhanced spatial transmission through stochastic resonance in an all-optical setting where the input signal, the noise, and the output signal are light beams.

We emphasize that the model of Section 2 does not stand as a quantitative and accurate model for the optical effect reported in Section 4. Stimulated Raman scattering is a complicated nonlinear phenomenon. Yet the simple model of Section 2 is able to capture, in a schematic way, a few essential nonlinear properties that, when they are present in one form or another, can constitute the basis for a stochastic resonance effect. This expectation was well justified by the results of the SRS experiment. Moreover, the stochastic resonance obtained with SRS, for the reasons discussed in Section 3, can be expected to exist also with other types of stimulated scattering and in other nonlinear media. In addition, materials that are known to exhibit a sharp change of transmission that depends on the laser intensity, for instance because of saturable and biphotonic absorption, could also lend themselves to stochastic resonance.

The present results, both the theoretical model and the experimental demonstration, contribute to extending the validity and usefulness of stochastic resonance. Also, they may lead to further developments and applications in nonlinear optics based on the possibility of extracting benefit from noise.

## REFERENCES

1. K. Wiesenfeld and F. Moss, "Stochastic resonance and the benefits of noise: from ice ages to crayfish and SQUIDS," *Nature (London)* **373**, 33–36 (1995).
2. A. R. Bulsara and L. Gammaitoni, "Tuning in to noise," *Phys. Today* **49**(3), 39–45 (1996).
3. R. Benzi, A. Sutera, and A. Vulpiani, "The mechanism of stochastic resonance," *J. Phys. A* **14**, L453–L458 (1981).
4. P. Debye, *Polar Molecules* (Dover, New York, 1929).
5. M. I. Dykman, D. G. Luchinsky, R. Mannella, P. V. E. McClintock, N. D. Stein, and N. G. Stocks, "Stochastic resonance in perspective," *Nuovo Cimento D* **17**, 661–683 (1995).
6. L. Gammaitoni, P. Hänggi, P. Jung, and F. Marchesoni, "Stochastic resonance," *Rev. Mod. Phys.* **70**, 223–287 (1998).
7. B. McNamara and K. Wiesenfeld, "Theory of stochastic resonance," *Phys. Rev. A* **39**, 4854–4869 (1989).
8. L. Gammaitoni, F. Marchesoni, E. Menichella-Saetta, and S. Santucci, "Stochastic resonance in bistable systems," *Phys. Rev. Lett.* **62**, 349–352 (1989).
9. M. I. Dykman, H. Haken, G. Hu, D. G. Luchinsky, R. Mannella, P. V. E. McClintock, C. Z. Ning, N. D. Stein, and N. G. Stocks, "Linear response theory in stochastic resonance," *Phys. Rev. A* **180**, 332–336 (1993).
10. J. J. Collins, C. C. Chow, and T. T. Imhoff, "Aperiodic stochastic resonance in excitable systems," *Phys. Rev. E* **52**, R3321–R3324 (1995).
11. F. Chapeau-Blondeau, "Noise-enhanced capacity via stochastic resonance in an asymmetric binary channel," *Phys. Rev. E* **55**, 2016–2019 (1997).
12. F. Chapeau-Blondeau and X. Godivier, "Theory of stochastic resonance in signal transmission by static nonlinear systems," *Phys. Rev. E* **55**, 1478–1495 (1997).
13. L. Gammaitoni, "Stochastic resonance and the dithering effect in threshold physical systems," *Phys. Rev. E* **52**, 4691–4698 (1995).
14. P. Jung, "Threshold devices: fractal noise and neural talk," *Phys. Rev. E* **50**, 2513–2522 (1994).
15. X. Godivier, J. Rojas-Varela, and F. Chapeau-Blondeau, "Noise-assisted signal transmission via stochastic resonance in a diode nonlinearity," *Electron. Lett.* **33**, 1666–1668 (1997).
16. F. Chapeau-Blondeau and X. Godivier, "Stochastic resonance in nonlinear transmission of spike signals: an exact model and an application to the neuron," *Int. J. Bifurcation Chaos* **6**, 2069–2076 (1996).
17. E. Simonotto, M. Riani, C. Seife, M. Roberts, J. Twitty, and F. Moss, "Visual perception of stochastic resonance," *Phys. Rev. Lett.* **78**, 1186–1189 (1997).
18. G. Boyd, *Nonlinear Optics* (Academic, Boston, Mass., 1992).
19. S. M. Bezrukov and I. Vodyanoy, "Stochastic resonance in non-dynamical systems without response thresholds," *Nature (London)* **385**, 319–321 (1997).
20. W. Kaiser and M. Maier, "Stimulated Rayleigh, Brillouin and Raman spectroscopy," in *Laser Handbook*, F. T. Arrechi and E. O. Schultz-Dubois, eds. (Elsevier, Amsterdam, 1972), Vol. 2, pp. 1089–1096.
21. J. Gazengel, N. P. Xuan, and G. Rivoire, "Stimulated Raman scattering thresholds for ultra-shot excitation," *Opt. Acta* **26**, 1245–1255 (1979).
22. S. Er. Rhaïmini, J. P. Lecoq, N. P. Xuan, G. Rivoire, and N. Tcherniega, "Amplitude object reconstruction by stimulated backward Raman scattering in the picosecond range with high efficiency conversion," *Opt. Commun.* **104**, 132–138 (1993).
23. R. Loudon, *The Quantum Theory of Light* (Oxford U. Press, Oxford, 1973).
24. B. Colombeau, C. Froehly, and M. Vampouille, "Fourier description of the axial structure of speckle," *J. Opt.* **10**, 65–69 (1979).
25. J. L. Ferrier, Z. Wu, J. Gazengel, N. P. Xuan, and G. Rivoire, "Backward scatterings in the picosecond range: generation and geometrical conditions for wave front reconstruction," *Opt. Commun.* **41**, 135–139 (1982).